NASA Technical Memorandum 84215

A Translational Velocity Command System for VTOL Low-Speed Flight

Vernon K. Merrick

March 1982

National Aeronautics and Space Administration

NASA Technical Memorandum 84215

A Translational Velocity Command System for VTOL Low-Speed Flight

Vernon K. Merrick, Ames Research Center, Moffett Field, California

National Aeronautics and
Space Administration

Ames Research Center
Moffett Field, California 94035

Nomenclature

A_e	engine nozzle exit area
A(s)	SRFIMF controller compensation transfer function
C_{D_y}	lateral drag coefficient at $\phi = 0$ (based on wing area)
C_{y_v}	dimensionless side force derivative $(-Y_v/\omega_o)$
F	engine gross thrust
g	acceleration due to gravity
G(s)	transfer function of lateral rigid-body mode
H(s)	transfer function of combined roll controller and aircraft
$H_D(s)$	denominator polynomial of H(s)
$H_N(s)$	numerator polynomial of H(s)
i_r	roll attitude flight controller output
i_ϕ	lateral flight controller output
j_o	constant
k,l,n	integers (or zero)
K_0	roll controller forward gain $(K_1 + K_2)$
K_1	roll controller forward gain component
K_2	roll controller forward gain component
K_9	lateral velocity controller coupling gain
K_B	control mode blending gain
K_v	lateral velocity feedback gain
K_v'	lateral controller compensator gain
K_ϕ	roll attitude feedback gain
$K_{\dot\phi}$	roll-rate feedback gain
L	turbulence scale parameter
$\dot m$	engine air mass flow
M	aircraft mass

N_y	number of times lateral displacement exceeds a given value
N_ϕ	number of times roll angle exceeds a given value
p_1	SRFIMF compensation pole
s	Laplace transform variable
s'	dimensionless Laplace transform variable (s/ω_o)
S	wing area
SRFIMF	state rate feedback model-following
t	time
T_o	ambient temperature
T_e	engine exhaust temperature
UC_{y_v}	upper bound of C_{y_v}
V_{w_y}	lateral wind velocity $(\bar{V}_{w_y} + \Delta V_{w_y})$
$\bar{V}_{w_y}$	mean lateral wind velocity
V_y	lateral velocity (inertial)
V_{y_c}	lateral velocity command
$\dot{V}_y$	lateral acceleration (inertial)
y_{ss}	steady state value of y
Y_v	lateral aerodynamic sideforce derivative
δ_{I_ϕ}	pilot input to lateral flight controller
ΔV_{w_y}	lateral gust velocity
$\Delta\phi$	incremental roll angle
$\Delta\phi_{ss}$	steady state value of $\Delta\phi$
ζ	damping ratio
λ	dimensionless turbulence parameter $(L\omega_0/\bar{V}_{w_y})$
ρ_o	ambient air density
ρ_e	density of engine efflux
σ_{w_v}	standard deviation of gust velocity

σ_y	standard deviation of y
σ_ϕ	standard deviation of $\Delta\phi$
τ_1, τ_2, τ_8	time constants
ϕ	roll angle
ϕ_T	trimmed roll angle
Φ_{w_v}	power spectral density of gust velocity
$\omega, \omega_0, \omega_1, \omega_2$	circular frequencies

A TRANSLATIONAL VELOCITY COMMAND SYSTEM FOR VTOL LOW SPEED FLIGHT

Vernon K. Merrick

Ames Research Center

SUMMARY

A translational velocity flight controller, suitable for very low speed maneuvering, is described and its application to a large class of VTOL aircraft from jet lift to propeller driven types is analyzed.

Estimates for the more critical lateral axis lead to the conclusion that the controller would provide a jet lift (high disk loading) VTOL aircraft with satisfactory "hands-off" station keeping in operational conditions more stringent than any specified in current or projected requirements. It also seems likely that ducted fan or propeller driven (low disk loading) VTOL aircraft would have acceptable hovering handling qualities even in high turbulence, although in these conditions pilot intervention to maintain satisfactory station keeping would probably be required for landing in restricted areas.

INTRODUCTION

It has been shown that a translational velocity command system, using attitude to orient the thrust vector, provides a low pilot workload, good ride quality approach to achieving precise station keeping and accurate low speed maneuvering of VTOL aircraft (ref. 1, 2).

In reference 2, a state rate feedback implicit model follower (SRFIMF) control concept was introduced and applied to the problem of providing translational velocity control. This work considered both techniques of thrust vector orientation, namely exhaust nozzle deflection with constant attitude and variable attitude with fixed exhaust nozzle. However, although block diagrams were presented in reference 2, showing how velocity command through attitude was achieved, the discussion did not include a theoretical justification for the particular transfer functions used in the feedback loops. Indeed, recent work has shown that the transfer functions given in reference 2 are not the best. This report provides the rationale for the structure of the velocity command system of reference 2, along with a derivation of the latest transfer functions and a performance analysis of the system when applied to a broad class of VTOL aircraft.

Although the treatment given here deals specifically with lateral velocity control through bank angle, the same general considerations and results hold for longitudinal velocity control through pitch angle.

CONTROL SYSTEM STRUCTURE

The basic structure of the combined lateral velocity control system and aircraft is shown in figure 1. The pilot's input, δ_{I_ϕ}, goes to a lateral velocity command controller whose output, i_ϕ, is the input to a roll attitude command controller. The output of the roll controller, i_r, goes to the actuators of the aircraft's rolling moment producers. Roll angle, rate and acceleration are measured and fed back to the roll controller. Aircraft roll and external disturbances induce lateral velocities, V_y, and accelerations, $\dot{V}_y$, which are measured and fed back to the lateral velocity command controller.

The most important feature of the control system structure is that it contains two separate and distinct sections, namely the roll command controller and the lateral velocity command controller. This arrangement is attractive because pure roll control modes, suitable for transition and conventional flight, may be obtained simply by bypassing the lateral velocity controller. This feature is employed in reference 2.

The detailed circuit diagram of the lateral velocity control system given in reference 2, figure 14, is reproduced in figure 2 in a simplified form appropriate to very low speed flight ($K_\beta = 0$). In this flight condition the gains K_1 and K_2 may

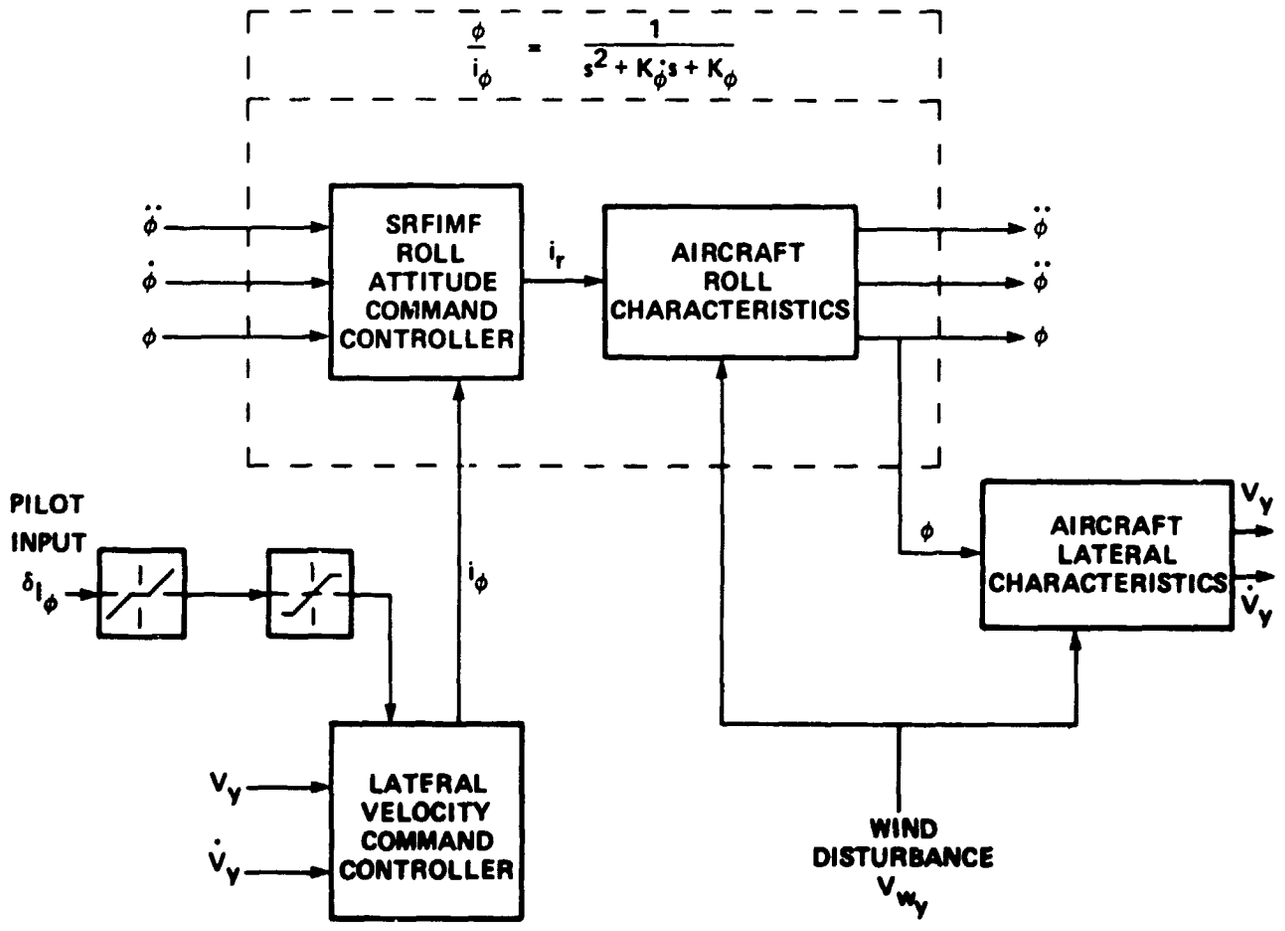

Figure 1.- Basic structure of lateral velocity control system.

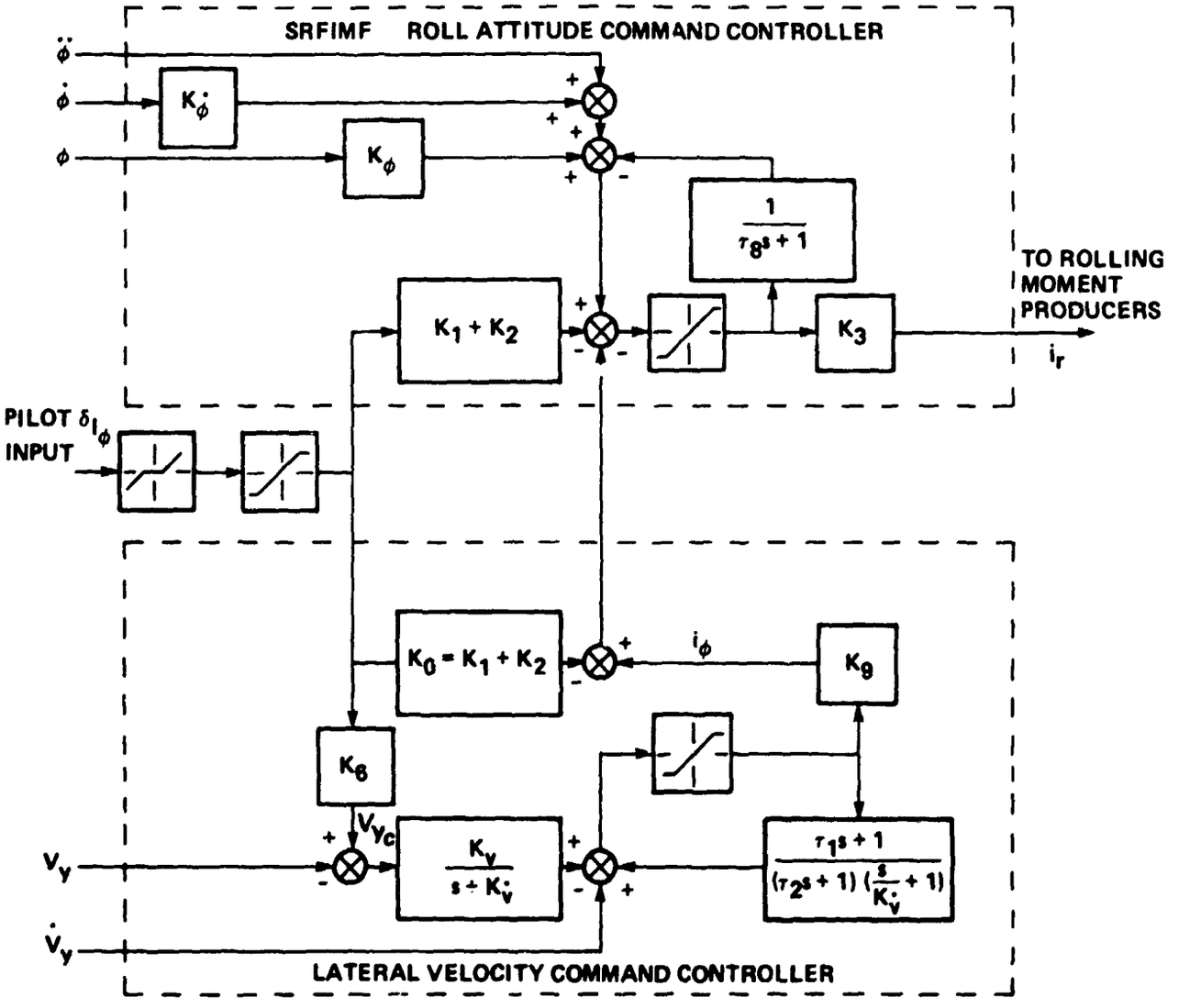

Figure 2.- Details of lateral velocity control system (see ref. 2 fig. 14).

be consolidated into a single gain ($K_1 + K_2$). Furthermore, the input from the stick to the roll controller is cancelled by an equal and opposite signal through the gain $K_0 = K_1 + K_2$. The only effective stick input is through the gain K_6 to the lateral velocity command controller, and the only effective input to the roll command controller is the output, i_ϕ, of the lateral velocity command controller. The situation is identical to that shown in figure 1.

When used in conjunction with the lateral velocity command controller, the purpose of the roll controller is to force the roll dynamics of the aircraft to approximate that of a selected second order model and to suppress the effects of external roll disturbances. It is shown in reference 2 that if K_3 (figure 2) is sufficiently large, then

$$\frac{\phi}{i_\phi} \approx \frac{1}{s^2 + K_{\dot{\phi}} s + K_\phi} \tag{1}$$

where ϕ aircraft roll angle

i_ϕ lateral velocity command controller output

$K_{\dot{\phi}}$ roll rate gain

K_ϕ roll attitude gain

s Laplace transform variable

In this report, the lateral velocity command circuit, shown in figure 2, is retained but henceforth the transfer function $K_v/(s + K_{\dot{v}})$ is replaced by a simple gain K_v and the transfer function $(\tau_1 s + 1)/[(\tau_2 s + 1)(s/K_{\dot{v}} + 1)]$ is replaced by a general function $A(s)$. A suitable form for $A(s)$ and the performance of the resulting control system when applied to VTOL aircraft, is given in the following analysis section.

ANALYSIS

The overall signal flow shown in figure 1 is completed through the "aircraft" block, which represents the relationship between roll attitude (and therefore thrust deflection) and the aircraft's lateral dynamics. A suitable linearized lateral equation of motion (see appendix) is;

$$(s - Y_v)V_y = g\Delta\phi + Y_v\Delta V_{w_y} \tag{2}$$

where V_y inertial lateral velocity

Y_v coefficient of lateral aerodynamic force (appendix)

ΔV_{w_y} lateral gust velocity

g acceleration due to gravity

Implicit in equation 2 is the assumption that the kinematic variables associated with all degrees of freedom other than roll and lateral translation, are controlled so as to remain essentially constant.

For the purpose of linear analysis, figures 1 and 2 may be combined and simplified (figure 3) into a form suggestive of the basic SRFIMF velocity controller shown in reference 2, figure 3. The block diagram labelled "aircraft" in figure 3 can be interpreted in a way which permits the analysis of reference 2 to be used. Thus, the transfer function $1/(s^2 + K_{\dot{\phi}} s + K_\phi)$, representing the combined dynamics of the roll controller and aircraft about the roll axis, can be viewed as a pseudo, second order control actuator driving a vehicle whose rigid body transfer function is $g/(s - Y_v)$. In the notation of reference 2

$$H(s) = \frac{1}{s^2 + K_{\dot{\phi}} s + K_\phi} \tag{3}$$

$$G(s) = \frac{g}{s - Y_v} \tag{4}$$

From equations 3 and 4, again using the notation of reference 3,

$$H_N(s) = 1$$

$$H_D(s) = s^2 + K_\phi' s + K_\phi$$

$$n = 2$$

$$k = 0$$

$$\ell = 1$$

$$j_o = 1$$

It follows from equation 20 of reference 2 that a suitable expression for $A(s)$ is:

$$A(s) = 1 - \frac{s(s + p_1)}{s^2 + K_\phi' s + K_\phi} \tag{5}$$

or

$$A(s) = \frac{s(K_\phi' - p_1) + K_\phi}{s^2 + K_\phi' s + K_\phi} \tag{6}$$

The equation representing the system shown in figure 3, taking into account the expression for $A(s)$ given in equation 6, is

$$\frac{s(s + p_1)}{g K_9} \left[(s - Y_v)\, V_y(s) - Y_v \Delta V_{w_y}(s)\right] = -(s + K_v)\, V_y(s) + K_v V_{y_c}(s) \tag{7}$$

If $\Delta V^s_{w_y}(s)$ and $V^s_{y_c}(s)$ are both step functions at $t = 0$, then multiplying each side of equation by s and applying the final value theorem shows that

$$\lim_{t \to \infty} V_y(t) = V^s_{y_c}(0^+) \tag{8}$$

Equation 8 shows that, in the steady state, the controlled variable $V_y(t)$ is equal to the commanded value $V^s_{y_c}(0^+)$ even in the presence of a steady disturbance $\Delta V^s_{w_y}(0^+)$. In other words the system is self-trimming in the presence of steady disturbances such as those due to steady winds.

The characteristic stability polynomial corresponding to equation 7 is,

$$s^3 + (p_1 - Y_v)\, s^2 + (g K_9 - p_1 Y_v)\, s + g K_9 K_v = 0 \tag{9}$$

NOTE: $V_{y_c} = K_6 \delta_{l_\phi}$

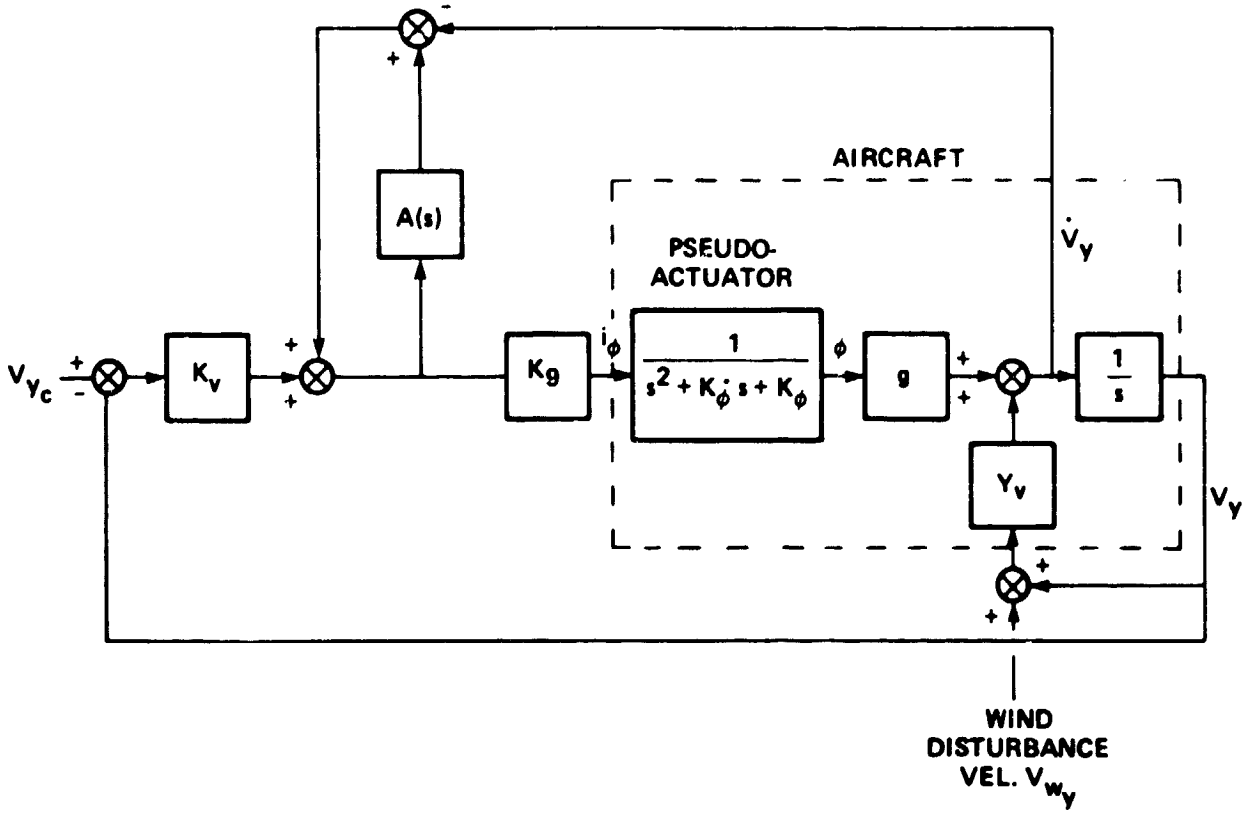

Figure 3.- Simplified lateral velocity control system.

Corliss and Dugan, in reference 1, studied two types of translational velocity control characteristics in a piloted simulation and concluded that the "binomial form" was the better of the two. This characteristic form is given below:

$$\frac{V_y}{V_{y_c}} = \frac{\omega_0^3}{(s + \omega_0)^3} \tag{10}$$

The system represented by equation 7 can be converted into the binomial form by equating coefficients of equation 9 and the denominator of the right-hand side of equation 10. This procedure gives the following expressions for the adjustable parameters p_1, K_v and K_9.

$$p_1 = 3\omega_0\left(1 - \frac{C_{y_v}}{3}\right) \tag{11}$$

$$K_v = \frac{\omega_0}{3}\left[\frac{\dot{i}}{1 - (1 - C_{y_v}/3)\, C_{y_v}}\right] \tag{12}$$

$$K_\phi = \frac{3\omega_0^2}{g}\left[1 - (1 - C_{y_v}/3)\, C_{y_v}\right] \tag{13}$$

where

$$C_{y_v} \triangleq -\frac{Y_v}{\omega_0} \tag{14}$$

It is shown in the appendix that a very broad class of VTOL aircraft, from propeller driven types to jet lift types, have values of C_{y_v} less than 0.2. It is of interest at this point to determine whether or not values of C_{y_v} of this magnitude need be considered in the selection of the control system parameters p_1, k_v and K_ϕ. If C_{y_v} is neglected in equations 11, 12 and 13 they take the following simple form.

$$p_1 = 3\omega_0 \tag{15}$$

$$K_v = \frac{\omega_0}{3} \tag{16}$$

$$K_\phi = \frac{3\omega_0^2}{g} \tag{17}$$

The question of the significance of C_{y_v} can be resolved by determining its effect on stability and control response assuming that p_1, K_v and K_ϕ are determined by equations 15, 16 and 17.

Stability

The characteristic stability polynomial (equation 9), with substitutions for p_1, K_v and K_ϕ from equations 15, 16 and 17 can be written in the following root locus form

$$1 + \frac{C_{y_v} s' (s' + 3)}{(s' + 1)^3} = 0 \tag{18}$$

where s' is the nondimensional Laplace Transform variable, s/ω_0.

The locus of roots of equation 18, as C_{y_v} varies, is shown in figure 4. It is apparent that the control system is stable for all positive, finite values of C_{y_v}. The three equal roots at $s' = -1$ ($s = -\omega_0$), when $C_{y_v} = 0$, become a pair of conjugate complex roots and a single real root representing a damped oscillatory mode and a damped aperiodic mode, respectively. The aperiodic mode becomes less well damped (higher time constant) as C_{y_v} increases. When $C_{y_v} = 0.1$, this time constant is doubled (from 1 to 2). However, doubling C_{y_v} to 0.2 causes a further increase of the time constant of only 23% (from 2 to 2.47).

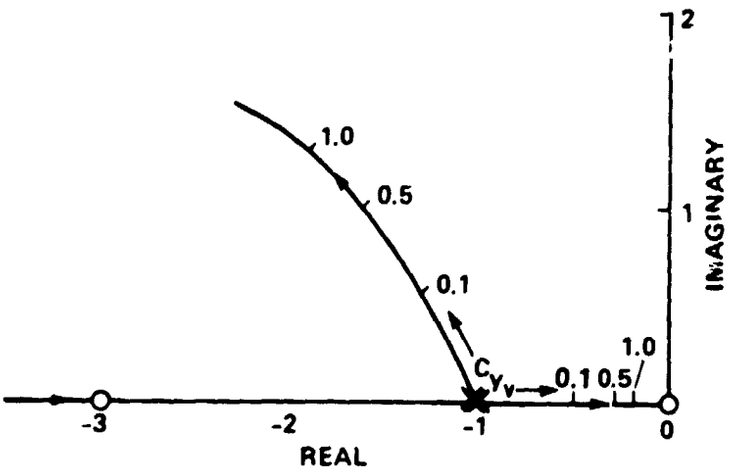

Figure 4.- Root locus of $1 + \dfrac{C_{y_v}\, s'\,(s' + 3)}{(s' + 1)^3} = 0$.

Response to pilot inputs

The transfer functions relating the lateral velocity, V_y, and the roll angle increments, $\Delta\phi$, to the pilot command, V_{y_c}, follow from equations 2 and 7,

$$\frac{V_y}{V_{y_c}} = \frac{1}{(s'^2 + 2\zeta\omega_1 s' + \omega_1^2)(s' + \omega_2)} \tag{19}$$

$$\frac{g\Delta\phi}{\omega_0 V_{y_c}} = \frac{s' + C_{y_v}}{(s'^2 + 2\zeta\omega_1 s' + \omega_1^2)(s' + \omega_2)} \tag{20}$$

where p_1, K_v and K_ϕ have been replaced by the quantities given in equation 15, 16 and 17, and

ω_1 nondimensional undamped frequency of the oscillatory mode

ζ damping factor of the oscillatory mode

ω_2 reciprocal of the time constant of the aperiodic mode

The quantities ω_1, ζ and ω_2 may be obtained from figure 4 as functions of C_{y_v}.

The responses of the aircraft's lateral velocity and roll angle increment to a step pilot command, $V^s_{y_c}$, are shown in figure 5. By far the most important of these step response characteristics is that of the lateral velocity, since it chiefly

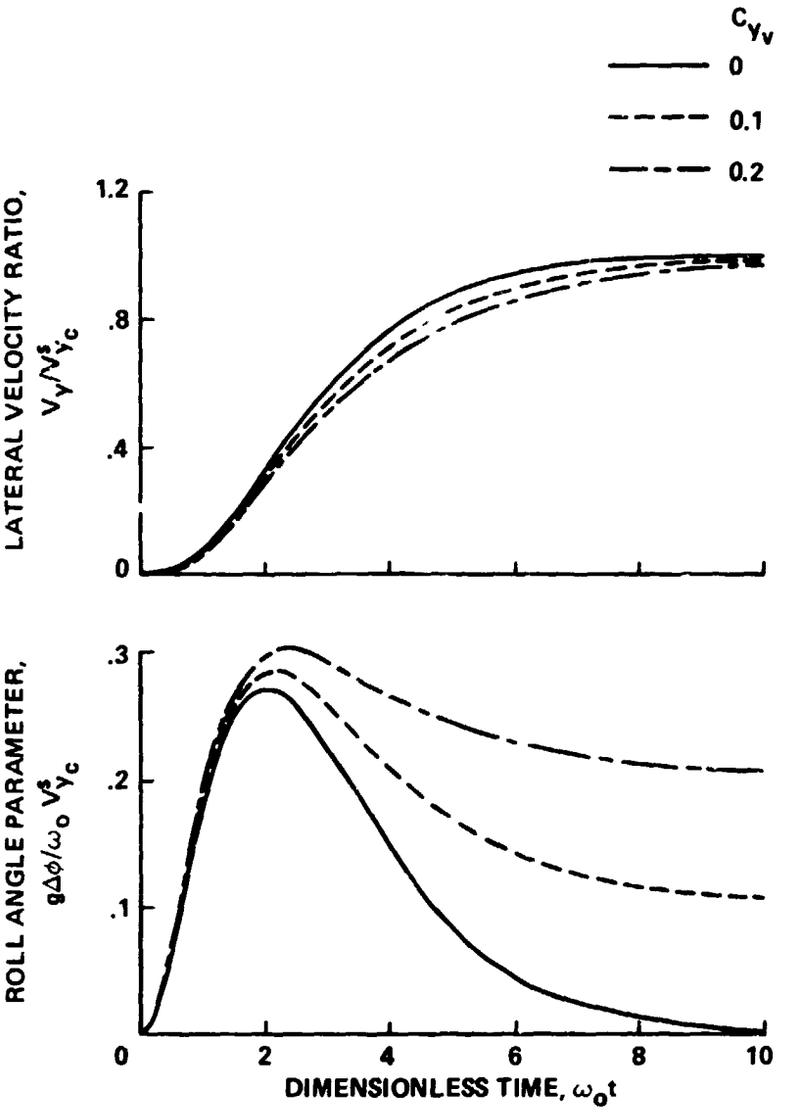

Figure 5.- Response to step pilot input.

influences the ease with which the pilot can perform maneuvers in hover. The pilot is unlikely to be sensitive to the roll angle characteristics provided the maximum roll angle attained during a maneuver is acceptable. Although there are significant variations in the roll angle characteristics as C_{y_v} increases, these are largely due to the changing static trim characteristics of the aircraft and would have been present even if the values of P_1, K_v and K_9 given in equations 11, 12 and 13 had been used. In fact, for any values of P_1, K_v and K_9 that provides a stable system

$$\Delta\phi_{ss} = -\frac{Y_v \Delta V^s_{y_c}}{g} \tag{21}$$

where $\Delta\phi_{ss}$ is the steady state value of $\Delta\phi$.

It is possible to evaluate the significance to the pilot of the effect of C_{y_v} on the lateral velocity response (figure 5) using data given in reference 1. For the more stringent rapid maneuver task, reference 2 (figure 8) shows a pilot rating of no greater than 2 over a range of values of ω_0 from 1.35 to 2.30. The lateral velocity responses to a step pilot input, for the system represented by equation 10, and for $\omega_0 = 1.35$ and $\omega_0 = 2.30$ are shown in figure 6. Presumably, smooth lateral response characteristics lying between these two curves would merit pilot ratings no greater than 2. Also shown in figure 6 are lateral responses for the system represented by equation 19 for $C_{y_v} = 0$ and $C_{y_v} = 0.2$, both with $\omega_0 = 1.85$. It follows that the pilot ratings for these two latter response characteristics are both no greater than 2, and therefore, the parameters p_1, K_v and K_θ can be set without regard to C_{y_v}.

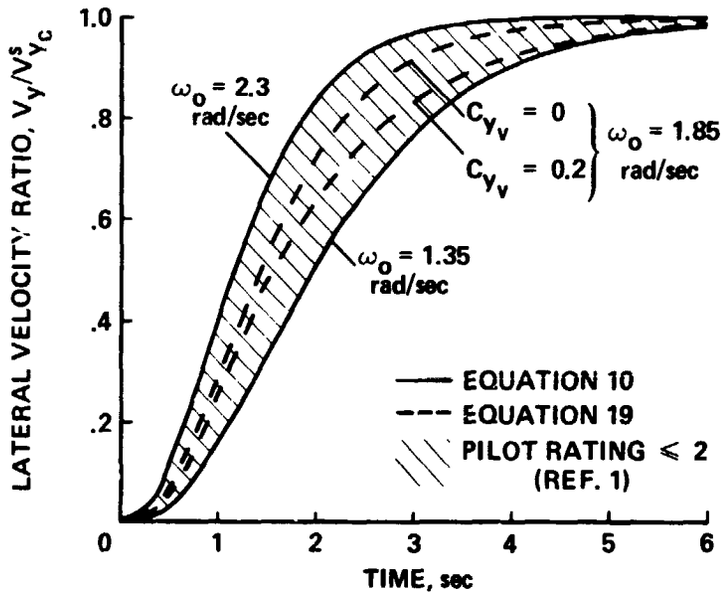

Figure 6.- Lateral velocity responses to step pilot inputs (comparison of equations 10 and 19).

Response to sharp edged gusts

The transfer functions relating the lateral translation and roll angle increment to the wind gust disturbance, ΔV_{w_y}, follow from equations 2 and 7.

These transfer functions are listed below:

$$\frac{\omega_0 y}{\Delta V_{w_y}} = \frac{-C_{y_v}(s' + 3)}{(s'^2 + 2\zeta\omega_1 s' + \omega_1^2)(s' + \quad)} \tag{22}$$

$$\frac{g\Delta\phi}{\omega_0 \Delta V_{w_y}} = \frac{C_{y_v}(3s' + 1)}{(s'^2 + 2\zeta\omega_1 s' + \omega_1^2)(s' + \omega_2)} \tag{23}$$

where, again, p_1, K_v and K_9 are given by equations 15, 16 and 17.

The responses of the aircraft's lateral position and roll angle increment to a step gust is shown in figure 7. The steady state lateral displacement, y_{ss}, is given by

$$y_{ss} = \frac{-3 C_{y_v} \Delta V_{w_y}}{\omega_0} \tag{24}$$

and the steady state roll angle increment, $\Delta\phi_{ss}$, by

$$\Delta\phi_{ss} = \frac{Y_v \Delta V_{w_y}}{g} \tag{25}$$

Although, as before, the steady state roll angle increment is independent of the control system parameters p_1, K_v and K_9, the steady state lateral displacement is dependent on them. In general, the steady state lateral displacement is given by

$$y_{ss} = \frac{-p_1 Y_v \Delta V_{w_y}}{\omega_0^3} \tag{26}$$

and if the exact value of p_1, from equation 11, is substituted in equation 26, it becomes

$$y_{ss} = \frac{-3 C_{y_v}\left(1 - \frac{C_{y_v}}{3}\right) \Delta V_{w_y}}{\omega_0} \tag{27}$$

For a value of C_{y_v} of 0.2, equations 24 and 27 give values of differing by only 7%, thereby again supporting the decision to neglect C_{y_v} in the calculation of the system parameters.

Response to turbulence

The effect of turbulence can be determined using the well-known results of generalized harmonic analysis (ref. 3). The relationship between the variance of the lateral displacement, σ_y, and the power spectral density of the turbulence, $\Phi_{w_v}(\omega)$, is

$$\sigma_y = \left[\int_0^\infty \Phi_{w_v}(\omega)\, T^2(\omega)\, d\omega\right]^{\frac{1}{2}} \tag{28}$$

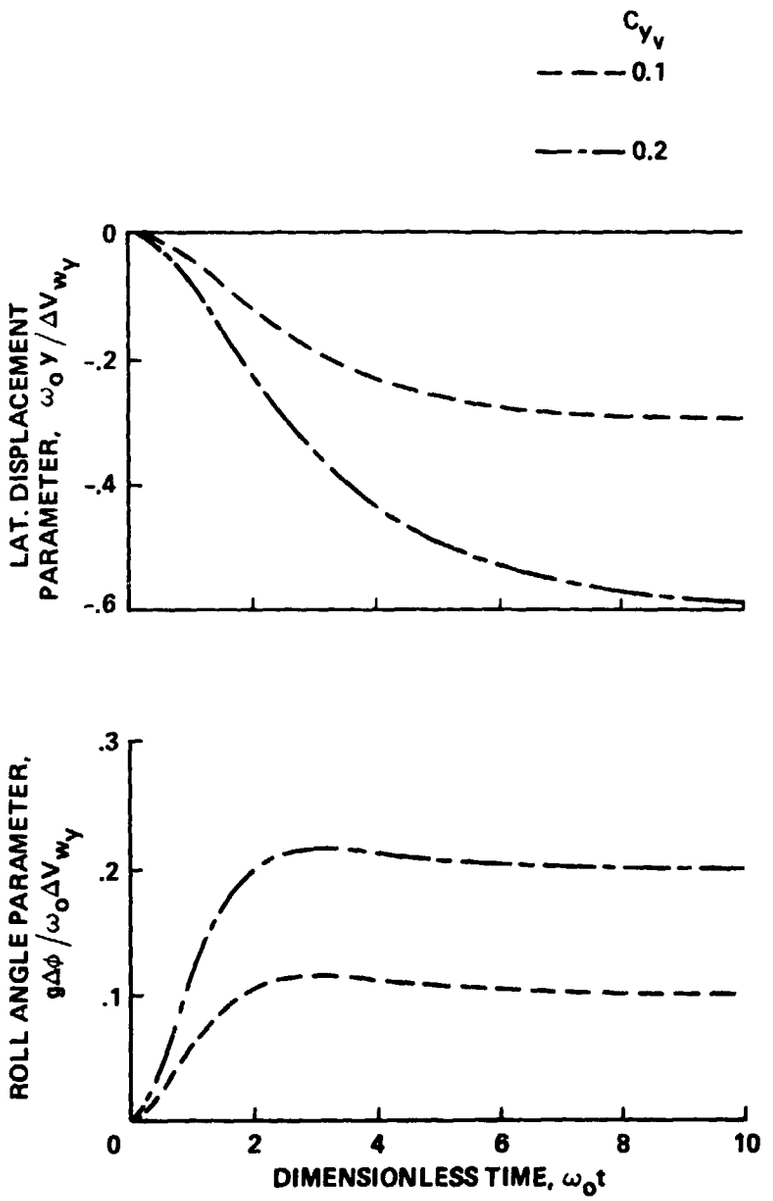

Figure 7.- Response to a step gust.

where $T(\omega)$ is the amplitude of the lateral displacement to unit sinusoidal gusts of frequency ω. An expression for $T(\omega)$ follows directly from equation 22; however, it eases the subsequent analysis if the denominator of equation 22 is approximated by $(s' + 1)^3$. The previous analysis provides sufficient justification for this approximation. It follows that

$$T^2(\omega') = \frac{C_{y_v}{}^2(\omega'^2 + 9)}{\omega_0{}^2(\omega'^2 + 1)^3} \tag{29}$$

where $\omega' = \omega/\omega_0$, and from equation 29 that

$$T^2(\omega') \leq \frac{9\,C_{y_v}^{\,2}}{\omega_0^{\,2}} \tag{30}$$

But since, by the definition of power spectral density,

$$\int_0^\infty \Phi_{w_v}(\omega')\, d\omega' = \sigma_{w_v}^{\,2} \tag{31}$$

(where σ_{w_v} is the variance of the turbulence) it follows, using equations 28 and 30, that

$$\sigma_y \leq \frac{3\,C_{y_v}\,\sigma_{w_v}}{\omega_0} \tag{32}$$

The same type of analysis, using equation 23, also shows that

$$\sigma_\phi \leq \frac{1.3\;C_{y_v}\,\omega_0\,\sigma_{w_v}}{g} \tag{33}$$

where σ_ϕ is the variance of the roll angle. The inequalities 32 and 33 are important in that they give upper bounds for σ_y and σ_ϕ that are independent of the spectrum and statistics of the turbulence. The question now is whether or not these upper bounds are unduly conservative, since the spectrum and statistics of turbulence are not arbitrary. A satisfactory answer to this question can be obtained by performing calculations using a plausible turbulence spectrum. The one adopted here is as follows.

$$\Phi_{w_v}(\omega) = \sigma_{w_v}\,\frac{2L}{\pi\,\bar{V}_{w_y}}\left[\frac{1}{1+\omega^2\left(\frac{L}{\bar{V}_{w_y}}\right)^2}\right] \tag{34}$$

where L is the scale of the turbulence. This expression was first derived by von Karman and Howarth (ref. 4) for isotropic turbulence parallel to the mean flow direction and has been shown to exhibit the general characteristics of measured spectra of atmospheric turbulence. Substituting equations 29 and 34 into equation 28 gives the following:

$$\sigma_y = \frac{\sigma_{w_v}\,C_{y_v}}{\omega_0}\left[\frac{2\lambda}{\pi}\int_0^\infty \frac{1}{(1+\omega'^2\lambda^2)}\;\frac{(\omega'^2+9)}{(\omega'^2+1)^3}\,d\omega'\right]^{1/2} \tag{35}$$

where $\lambda = L\omega_0/\bar{V}_{w_y}$ is a dimensionless turbulence parameter. When the integral in equation 35 is evaluated, the final expression is,

$$\sigma_y = \frac{\sigma_{w_v} C_{y_v}}{\omega_0} \left[\frac{(18\lambda^2 + 21\lambda + 7)\lambda}{2(\lambda + 1)^3} \right]^{\frac{1}{2}} \tag{36}$$

The variation of $\omega_0 \sigma_y / C_{y_v} \sigma_{w_y}$ with λ is shown in figure 8. The corresponding equation for the variance of the roll angle is

$$\sigma_\phi = \frac{\sigma_{w_v} C_{y_v} \omega_0}{g} \left[\frac{(2\lambda^2 + 9\lambda + 3)\lambda}{2(\lambda + 1)^3} \right]^{\frac{1}{2}} \tag{37}$$

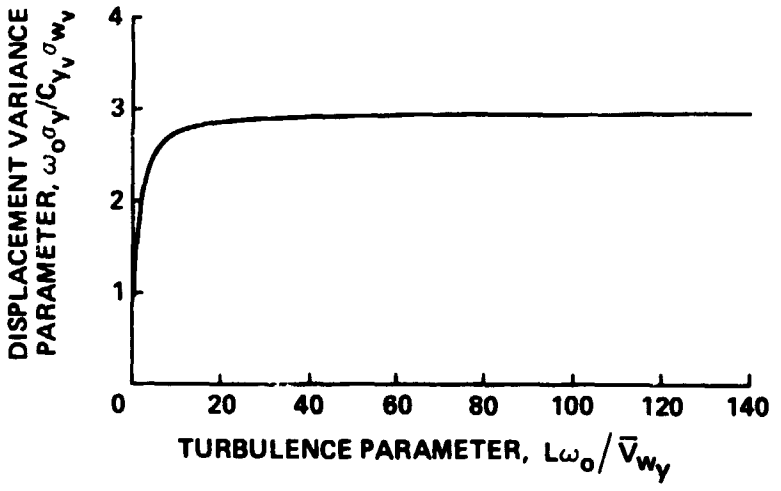

Figure 8.- Variation of displacement variance parameter with turbulence parameter.

The variation of $g\sigma_\phi / C_{y_v} \omega_0 \sigma_{w_y}$ with λ is shown in figure 9. Assuming the minimum turbulence scale length, L, to be 100 m, the maximum wind speed to be 18m/sec (35 kt) and an ω_0 of 1.85 rad/sec gives a practical minimum for λ of about 10. It follows from figures 8 and 9 that for all practical purposes the inequalities in expressions 32 and 33 can be deleted.

It is of interest to continue the analysis using the specific turbulence spectra to find the frequency of lateral displacements and roll angles exceeding given values of these quantities. Assuming that the turbulence is a Gaussian process, this frequency N_y can be obtained from Rice's formula (refs. 3, 5); thus for the lateral displacement

$$N_y = N_{0y} e^{-y^2/2\sigma_y^2} \tag{38}$$

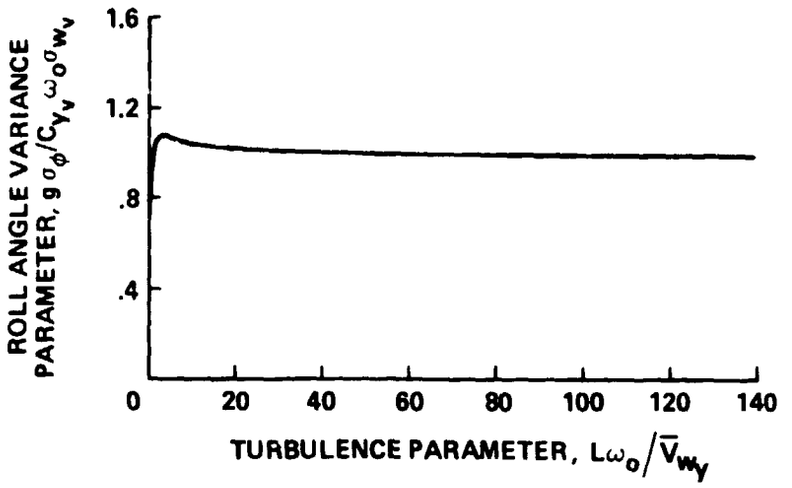

Figure 9.- Variation of roll angle variance parameter with turbulence parameter.

where

$$N_{o_y} = \frac{1}{2\pi}\left[\frac{\int_0^\infty \omega^2\,\Phi_{w_v}(\omega)\,T^2(\omega)\,d\omega}{\int_0^\infty \Phi_{w_v}(\omega)\,T^2(\omega)\,d\omega}\right]^{\frac{1}{2}} \tag{39}$$

Substituting equations 29 and 34 into equation 39 and evaluating the integrals gives the following expression for N_{o_y}

$$N_{o_y} = \frac{1}{2\pi}\left(\frac{18\lambda^2 + 21\lambda + 7}{7\lambda + 3}\right)^{\frac{1}{2}} \tag{40}$$

The expressions for roll angle corresponding to equations 38 and 40 are

$$N_\phi = N_{o_\phi} e^{-\Delta\phi^2/2\sigma_\phi^2} \tag{41}$$

and

$$N_{o_\phi} = \frac{1}{2\pi}\left(\frac{2\lambda^2 + 9\lambda + 3}{3\lambda + 7}\right)^{\frac{1}{2}} \tag{42}$$

The variations of $1/N_y$ with y/σ_y and $1/N_\phi$ with $\Delta\phi/\sigma_\phi$ are shown in figures 10 and 11. The quantity $1/N_y$ (or $1/N_\phi$) may be interpreted as the average time interval between periods where the lateral displacement (or roll angle) exceeds given values.

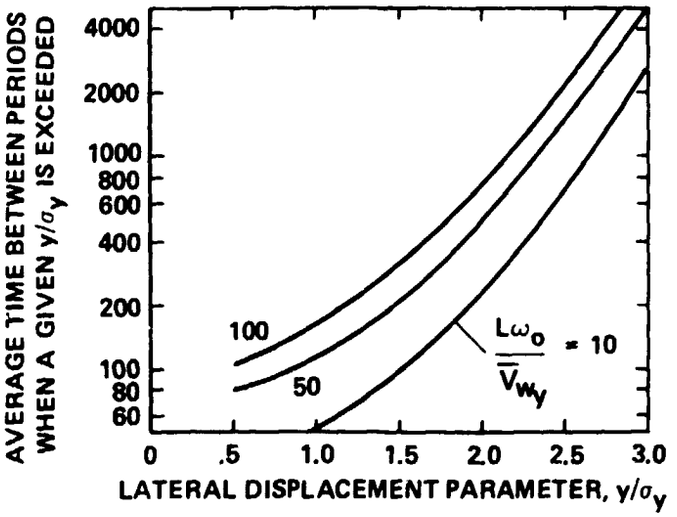

Figure 10.- Average time between periods when a given y/σ_y is exceeded.

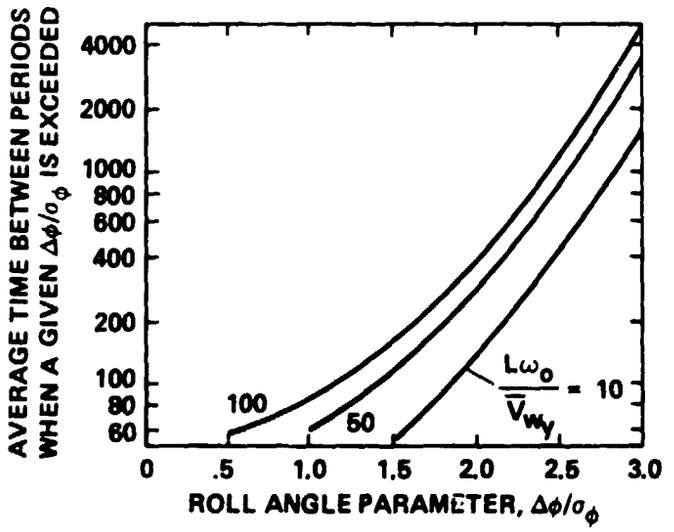

Figure 11.- Average time between periods when a given $\Delta\phi/\sigma_\phi$ is exceeded.

DISCUSSION

The translational velocity controller concept introduced in this report, although related to the SRFIMF controllers of reference 2, is not a "model follower." A characteristic of a true model follower is that the response of the controlled system approaches that of the model as the coupling gain (for example K_9 in figure 3) increases. The translational velocity controller does not satisfy this

criterion, because a specific value of K_9 (equation 17) is required to achieve the desired dynamic characteristics (equation 10). However, the translational controller is controlling an aircraft whose roll characteristics have been rendered both specific and invariant by a model following (SRFMF) controller. It is unnecessary to employ model follower techniques in the design of the translational velocity controller. Although the translational velocity controller is strongly dependent on the roll controller, this dependence is explicit only in the transfer function $A(s)$ and even this is a simple function of K_ϕ and $K_{\dot{\phi}}$. It is simple to change the characteristics of one controller independently of the other. Specifically, K_ϕ and $K_{\dot{\phi}}$ govern the characteristics of the roll controller and p_1, K_v and K_9 those of the translational velocity controller.

It was demonstrated earlier, that using an ω_0 of 1.85 rad/sec gave VTOL aircraft within a broad class, control characteristics which, according to the data of reference 2, would merit pilot ratings no greater than 2. With $\omega_0 = 1.85$ rad/sec the corresponding values of the control parameters are $p_1 = 5.55$ rad/sec, $K_v = 0.617$ rad/sec and $K_9 = 1.046$ rad^2/m (0.319 rad^2/ft). Furthermore, figure 5 shows that with $C_{y_v} = 0.1$, the lateral velocity following a step command reaches 90% of its final value in 3.30 sec and the maximum roll angle per meter/sec of the command is 3.08 deg and occurs 1.19 sec after the step command. These numbers are typical of this type of control system.

The control system has been incorporated into a mathematical model of an AV-8A Harrier (reference 6). This model includes a good representation of the reaction control system including limits and nonlinearities. The response of the aircraft in hover, to a lateral velocity command of 6 m/sec into a sidewind of 20 m/sec is shown in figure 12. This is a severe test of the control system and exceeds the operational limits quoted for the aircraft. Not only is the maximum operational sidewind permitted only 30 knots (15 m/sec), but the pilot would never roll the aircraft into a wind of this magnitude. The fact that the mathematical model permits such a maneuver casts doubts on the accuracy of the aerodynamic assumptions at these flight conditions. However, the results show that the system performs as expected and handles lateral control saturation satisfactorily.

If the pilot is performing a precise station keeping task, a self-trimming feature is effective in reducing the pilot workload. Such a self-trimming system maintains zero velocity with zero control input even in the presence of a sidewind. Furthermore, it is important that such a self-trimming system be fast acting so that turbulence does not disturb the position of the aircraft to the point that the pilot has to continually reposition it. It is clear from the formulation of the control system that it is self-trimming (equation 8). Some idea of the sensitivity of lateral displacement and roll angle to turbulence may be obtained from equations 32 and 33 and figures 10 and 11. In the case of an AV-8A Harrier, C_{y_v} is about 0.05 (assuming $\omega_0 = 1.85$) and the variance of the lateral displacement, σ_y, and roll angle, σ_ϕ, in turbulence of 3 m/sec (9.84 ft/sec) variance is about 0.23 m (0.74 ft) and 0.22 deg respectively. The corresponding numbers for a low disc loading aircraft ($C_{y_v} = 0.2$) are four times larger.

The average time between periods when given values (in terms of variance) of either the lateral displacement or roll angle is exceeded is independent of C_{y_v} and, therefore, of wing loading and disc loading. It can be seen from figure 10 that, under the worst conditions ($L\omega_0/\bar{V}_{w_y} = 10$), the time between periods where the lateral displacement exceeds $3\sigma_y$ is about 43 min. The corresponding time for the roll angle (figure 11) is 27 min. Since the average hovering period during a vertical landing is less than 1 min, a period during which the lateral displacement

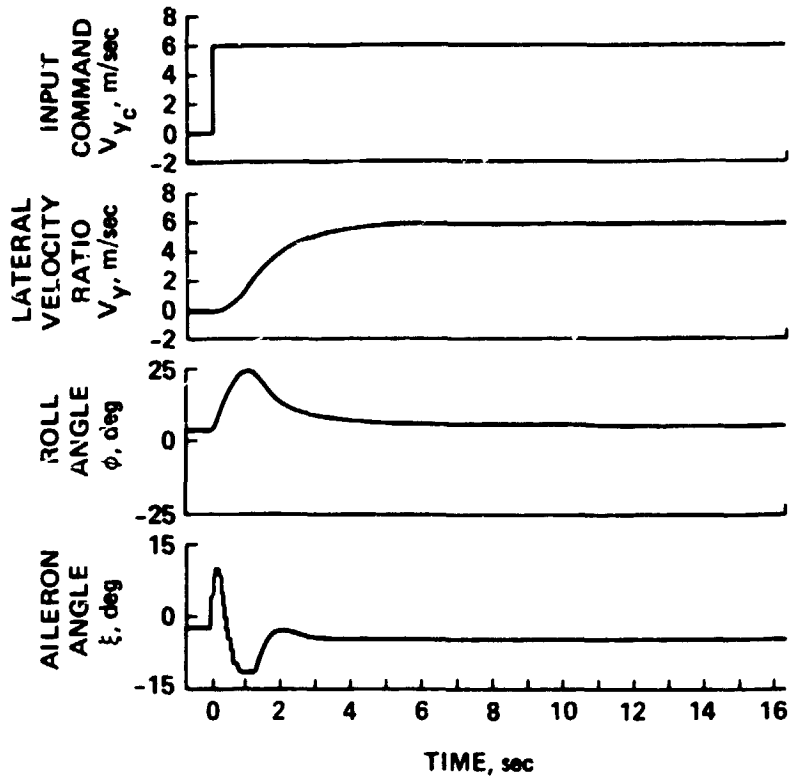

Figure 12.- Response of AV-8A model to a lateral velocity command of 6 m/sec into a 20 m/sec sidewind.

exceeds $3\sigma_y$ should occur only once every 45 landings. Periods during which the roll angle exceeds $3\sigma_\phi$ should occur once every 30 landings.

From the previous analysis it may be conjectured that a vehicle with high wing loading and disc loading (C_{y_v} = 0.05) should exhibit satisfactory (pilot rating $\leq 3\frac{1}{2}$) "hands off" station keeping in heavy turbulence even in the most stringent obstacle clearance situation. In the case of the low wing loading and disc loading aircraft (C_{y_v} = 0.2) the situation is less clear. The station keeping characteristics would probably be acceptable in situations where obstacle clearance is not a factor. However, in a stringent obstacle clearance situation the pilot would probably have to intercede to maintain acceptable station keeping. In this case pilot acceptance would depend strongly on his workload and the quality of his visual cues. The evaluation of such factors is outside the scope of this report.

CONCLUSIONS

A conceptually simple translation velocity flight controller, suitable for VTOL aircraft operating in the hover and very low speed flight regime, is proposed. This controller, although not a model follower, is related to the state rate feedback implicit model follower (SRFIMF) concept. The controller is designed to operate in conjunction with a model following attitude controller.

The controller provides overall system dynamic characteristics that closely approximate the binomial form investigated by Corliss and Dugan (ref. 1). For all practical purposes the controller parameters are related solely to the selected characteristic frequency of the binomial form. Furthermore, this relationship is particularly simple and holds for a broad class of VTOL aircraft from jet-lift to propeller types.

Estimates for the more critical lateral axis indicate that any VTOL aircraft equipped with the controller would experience, on the average, only one period in every 45 landings wherein the lateral displacement exceeds the three sigma value. In turbulence of 3 m/sec (9.84 ft/sec) variance, the three sigma lateral displacement for a jet-lift VTOL (AV-8A Harrier) would be about 0.69 m (2.12 ft) and for a propeller driven VTOL aircraft could be as high as 2.76 m (8.48 ft). It is concluded that the controller would provide a jet-lift VTOL aircraft with satisfactory "hands off" station keeping in operational conditions more stringent than any current or projected requirements. It is likely that ducted fan or propeller driven VTOL aircraft would have acceptable hovering handling qualities even in high turbulence, although in these conditions the "hands off" station keeping would be inadequate for landing in very restricted areas, such as a destroyer landing pad. For these moderate and low disc loading aircraft there is, therefore, a relationship between pilot workload on the one hand and degree of turbulence and station keeping accuracy on the other. To investigate this relationship requires a series of piloted moving base simulations.

APPENDIX

The Lateral Equation of Motion and an Estimate of the Lateral Side Force

If it is assumed that the roll angle is small, and that only roll angle and lateral translation are allowed to vary, then an acceptably accurate lateral equation of motion is

$$M \dot{V}_y = M g \phi - F_y \tag{A1}$$

where $\dot{V}_y$ lateral acceleration relative to an earth fixed reference frame

M mass of aircraft

F_y lateral force due to aerodynamic effects on the airframe and propulsion system.

The aerodynamic force F_y can be expressed in the following form

$$F_y = -\frac{1}{2} \rho_o S(V_y + V_{w_y})^2 C_{D_y} - \dot{m}(V_y + V_{w_y}) \tag{A2}$$

where C_{D_y} lateral drag coefficient of the aircraft at $\phi = 0$ (based on wing area S)

$\dot{m}$ air mass flow through the propulsion system

V_{w_y} lateral wind speed, positive when <u>from</u> the positive y direction

ρ_o ambient air density

S wing area (reference area for C_{D_y})

Linearizing equations A1 and A2 about a trimmed hover point ($V_y = 0$) gives the following equation of motion for small perturbations.

$$\dot{V}_y - Y_v V_y = g \Delta \phi + Y_v \Delta V_{w_y} \tag{A3}$$

where

$$Y_v \triangleq -\frac{(\rho_o S C_{D_y} \bar{V}_{w_y} + \dot{m})}{M} \tag{A4}$$

and $\bar{V}_{w_y}$ steady wind speed

ΔV_{w_y} wind gust speed

The quantity $\Delta\phi$ is the roll perturbation about the trim roll angle ϕ_T, where

$$\phi_T = -\frac{\left(\frac{1}{2}\rho_o S C_{D_y} \bar{V}_{w_y}^2 + \dot{m}\bar{V}_{w_y}\right)}{Mg} \tag{A5}$$

What is now required is a rough assessment of the magnitude of Y_v in terms of the gross parameters of VTOL aircraft. This can be achieved using equation A4 provided some rather crude, but plausible, assumptions are made.

If it is assumed that the static pressure in the propulsion system efflux, at the nozzle exit, ρ_e, is equal to the ambient atmospheric pressure, ρ_o, then standard momentum theory, applied to the hover condition, provides the following relationship between mass flow and thrust:

$$\dot{m} = \sqrt{\rho_e A_e F} \tag{A6}$$

where F gross thrust

A_e total area of the exit jets

ρ_e air jet density at the nozzle exit

Since, in hover, $F = Mg$, equation A6 becomes

$$\frac{\dot{m}}{M} = \frac{g\sqrt{\rho_o}\sqrt{\frac{\rho_e}{\rho_o}}}{\sqrt{\frac{F}{A_e}}} \tag{A7}$$

It follows from the equation of state that

$$\frac{\rho_e}{\rho_e T_e} = \frac{\rho_o}{\rho_o T_o} \tag{A8}$$

and since it has been assumed that $\rho_e = \rho_o$ it follows from equation A8 that

$$\frac{\rho_e}{\rho_o} = \frac{T_o}{T_e} \tag{A9}$$

Since, in general, $T_o/T_e < 1$, it follows from equation A9 that $\rho_e/\rho_o < 1$ and from equation A7, that

$$\frac{\dot{m}}{M} < \frac{g\sqrt{\rho_o}}{\sqrt{\frac{F}{A_e}}} \tag{A10}$$

Inequality A10 provides an upper bound for the specific mass flow $\dot{m}/M$ used in equation A5, in terms of the disc loading F/A_e.

To make further progress it is necessary to select a plausible upper bound for the lateral drag coefficient of the aircraft, C_{D_y}. A reasonable assumption is that this drag coefficient, if it were based on fuselage side area, is unlikely to exceed that of a flat plate, or about unity. Further, an examination of various fixed wing VTOL aircraft, including some conceptual designs, indicates that the ratio of wing area to fuselage side area (including the vertical fin) is also roughly unity. It follows that a reasonable upper bound for C_{D_y} is unity. This assumption, along with inequality A10, provides the following expression for an upper bound of C_{y_v} (denoted by UC_{y_v}), in terms of wing loading and disc loading and based on definitions 14 and A4.

$$C_{y_v} < UC_{y_v} = \frac{g}{\omega_o}\left[\frac{\rho_o V_{w_y}}{\frac{F}{S}} + \frac{\sqrt{\rho_o}}{\sqrt{\frac{F}{S}}}\right] \qquad \text{(A11)}$$

Attention is given to C_{y_v}, rather than Y_v, because this is the fundamental non-dimensional quantity influencing the control dynamics (see equations 11, 12 and 13).

Shown in figure 13 are variations of wing loading with disc loading for constant values of UC_{y_v} from 0.05 to 0.2. These calculations were carried out assuming a value of ω_o of 1.85, determined from reference 1 as being optimum, and for a value of sidewind velocity of 35 kt (see reference 7 table 1). Also shown in figure 13 are the ranges of wing loadings and disc loadings for several fixed wing VTOL aircraft. It can be seen that all aircraft with wing loadings greater

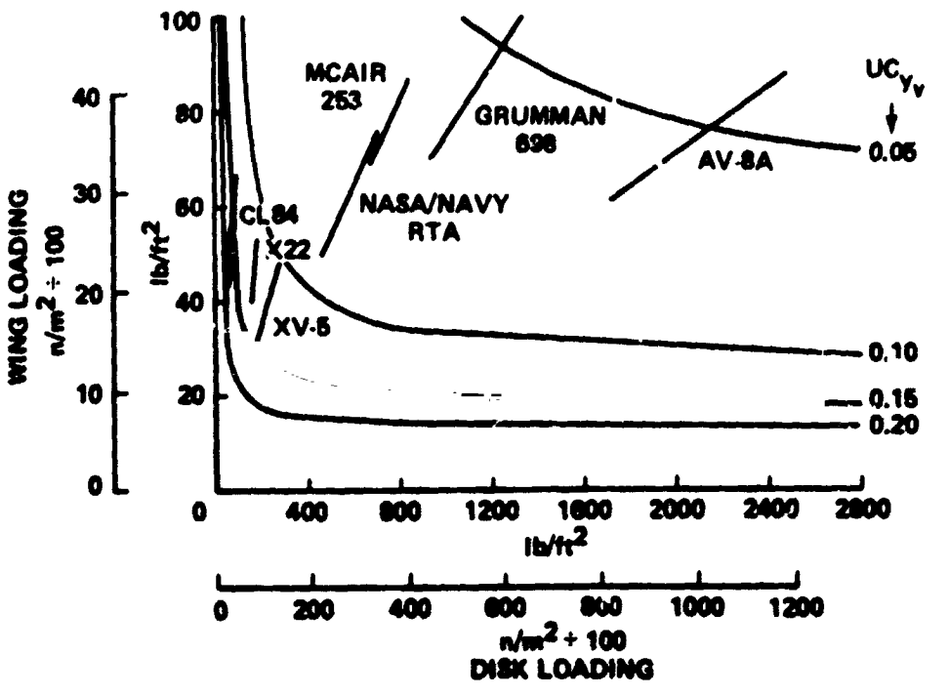

Figure 13.- Wing loading and disc loadings for given values of UC_{y_v}.

than 2000 n/m^2 (42 lb/ft^2) and disc loadings greater than 20000 n/m^2 (400 lb/ft^2) have values of UC_{y_v}, and therefore of C_{y_v}, less than 0.1. This broad class of aircraft includes all the lift-fan VTOL concepts studied by NASA after 1970 and the AV-8 Harrier but does not include low disc loading lift-fan aircraft (XV-5), ducted propeller aircraft (X-22) or tilt wing aircraft (CL-84). However, these relatively low disc loading aircraft should have values of C_{y_v} less than 0.2

REFERENCES

1. Corliss, Lloyd D.; and Dugan, Daniel C.: A VTOL Translational Rate Control System Study on a Six-Degree-of-Freedom Motion Simulator. NASA TM-62194, October 1972.

2. Merrick, Vernon K.: Study of the Application of an Implicit Model-Following Flight Controller to Lift-Fan VTOL Aircraft. NASA TP-1040, June 1977.

3. Press, Harry; and Meadows, May T.: A Reevaluation of Gust-Load Statistics for Applications in Spectral Calculations. NASA TN-3540, August 1955.

4. von Karman, T.; and Howarth, L.: On the Statistical Theory of Isotropic Turbulence. Proceedings, Royal Society of London, Series A, 164, 192, 1938.

5. Tsien, H. S.: Engineering Cybernetics. McGraw Hill, Pages 126-127.

6. Nave, R. L.: A Computerized VSTOL/Small Platform Landing Dynamics Investigation Model. NADC-77024-30, September 1977.

7. Anon.: Military Specification, Flying Qualities of Piloted VSTOL Aircraft. MIL-F-83300.